IMK-14 – Istraživanje i razvoj u teškoj mašinogradnji 25(2019)3, SR 69-74
UDC 621 ISSN 0354-6829

Analiza naponsko-deformacionog stanja vratila pogonskog bubnja

Milan P. Vasić[1], Zorica D. Đorđević[1], Mirko Ž. Blagojević[1*]
[1]Univerzitet u Kragujevcu, Fakultet inženjerskih nauka, Kragujevac (Srbija)

U okviru ovog rada izvršena je analiza naponsko-deformacionog stanja vratila karakterističnih pogonskih bubnjeva na trakastim transporterima površinskog kopa Drmno. Oblik i mere vratila definisane su na osnovu originalne tehničke dokumentacije, a provera naponskog stanja izvršena je primenom metode konačnih elemenata u softverskom paketu Catia. Opterećenja su simulirana za realne radne uslove u eksploataciji. Rezultati analize su pokazali da najbolju raspodelu opterećenja imaju vratila sa konusom između steznog prstena i ležaja, i da glavčine oblika" T" najpovoljnije prenose opterećenja na vratilo. Takođe, analize su pokazale da vrednosti napona nastalih u vratilima na mestu otkaza nisu dovoljno velike da bi dovele do oštećenja vratila preopterećenjem i da uzrok otkaza treba tražitiu zamoru, zatim u plastičnim deformacijama, zaostalim naponima posle reparacije vratila i neuravnoteženosti mase bubnja.

Keywords: Pogonski bubnjevi, Vratila, Analiza napona i deformacija

1. UVOD

Pokretanje trake na trakastim transporterima ostvaruje se pomoću jednog ili više pogonskih bubnjeva, gde između ostalog posebnu ulogu i značaj imaju vratila. Ona primaju celokupna opterećenje od transportnih traka i pogonskih jedinica, a oslonjena su samo na dva radiaksijalna ležaja.

Uobičajeno, pogonski bubanj, kao složeni tehnički sistem (Slika 1), sastoji se od: glavčine (1), plašta (2), obloge (3), vratila (4), steznog prstena (5), kućišta ležaja (6), ležaja (7), krute spojnice (8) ili neke druge veze sa reduktorom.

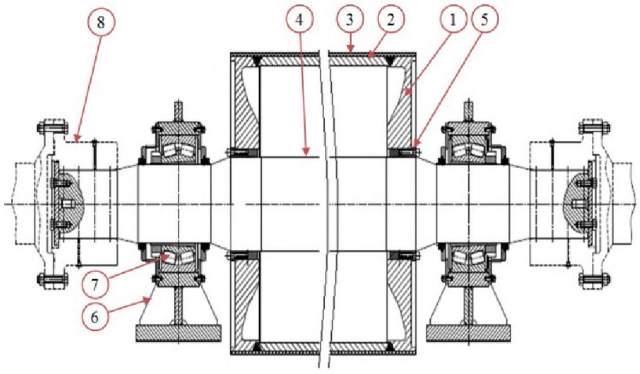

Slika 1: Osnovne komponente pogonskog bubnja

Tokom višegodišnje eksploatacije, na PK Drmno dolazilo je do pojave prslina i pukotina u strukturi vratila na pogonskim stanicama, što je za posledicu imalo zastoj sistema. Pomenuta oštećenja najčešće su locirana u zoni između glavčine bubnja i ležaja.

Svaki zastoj ovakvog sistema donosi visoke finansijske gubitke, a naročito se negativno odražavaju ugljeni sistemi na funkcionisanje termoelektrana, tako što stvaraju probleme u dostavi pogonskog goriva elektrananama. Ako termoelektrana i rudnik nemaju rezevni način dostavljanja uglja u određenoj količini i određenim tempom, uzastopni zastoji sistema mogu prouzrokovati ispadanje čitavog bloka elektrane iz električne mreže.

Literaturna istraživanja su pokazala, da pored izrazitih diskontinuiteta u veličinama poprečnog preseka, na vek trajanja vratila utiče i dizajn glavčine bubnja.

King je na osnovu velikog broja analiza, predložio upotrebu glavčina oblika T u odnosu na L, jer se minimiziraju troškovi obrade uz istovremeno smanjenje naprezanja zavarenih spojeva [1].

Pol i *Jadhav* su vršili optimizaciju vrednosti radijusa zaobljenja vratila na mestu prelaska sa prečnika na kome naleže stezni prsten na prečnik naleganja ležaja, kao i vrednosti debljine zida plašta. Na taj način, za vratilo ⌀ 100 *mm*, smanjili su vrednost napona za 9% [2].

Oscar i *Hussain* su analizirali naprezanje bubnja na rotornom bageru [3]. Uspeli su da smanje vrednost napona vratila ravnomernijom raspodelom opterećenja koja se postiže ubacivanjem više srednjih diskova (oslonaca) unutar bubnja.

Grupa autora je proučavala otkaz varova na bubnju i primenu nužnih ojačanja između glavčine i plašta [4]. Zaključili su da početno opterećenje može biti presudno na životni vek bubnja.

Na osnovu pregleda literature, može se zaključiti da postoji međusobna zavisnost komponenti bubnja, jer se sva opterećenja redukuju na vratilo.

Takođe, ne treba izuzeti, da na životni vek vratila utiče i nepravilna montaža. Svaki poremećaj centričnosti, makar on bio i veoma mali, dovodi do cikličnog naprezanja, odnosno prevremenog zamora. Pored toga, ne treba zanemariti i veliko zatezanje, koje se vrši kada traka prokliza oko pogonskog bubnja.

Stoga, cilj ovog rada je analiza pojedinačnih stanja napona i deformacija vratila za tipove pogonskih bubnjeva koji su najčešće zastupljeni na PK Drmno i ukazivanje na potencijalne nedostatke, kao i na dobra rešenja koja treba primenjivati pri izgradnji novih sistema.

Uporedna modalna analiza vratila izvršena je za dva dominantna tipa pogonskih bubnjeva čije su komponente modelirane na osnovu originalne tehničke dokumentacijeu softveru *Catia*.

*Kontakt adresa autora: Fakultet inženjerskih nuka Univerziteta u Kragujevcu, Kragujevac, Sestre Janjić 6, Srbija, mirkob@kg.ac.rs

2. OPIS OŠTEĆENJA

Do loma vratila može doći usled preopterećenja, plastičnih deformacija ili zamora, a svaka vrsta loma je određena izgledom prelomne površine, [5].

U slučaju preopterećenja, pukotina se razvija konstantno, a površina loma je relativno gruba.

U slučaju loma vratila izazvanog zamorom, brzina rasta prsline nije konstantna, pa je površina loma relativno glatka-mat, a završni lom je relativno grub, krupnozrnast i hrapav, [6,7].

Primer takvog loma prikazan je na Slici 2. Vizualnim pregledom uočava se karakteristični deo površine loma, nazvan zona A, koji je hrapav i predstavlja krajnji lom koji je nastao kada se površina poprečnog preseka toliko smanjila, da više nije mogla da prenese nominalno opterećenje. Ostatak prelomne površine je gladak.

U principu, lomovi koji nastaju usled naprezanja na savijanje su normalni na osu vratila, baš kao na Slici 2, dok lomovi nastali kao posledica torzionog naprezanja, često su postavljeni pod uglom od 45° prema osi vratila.

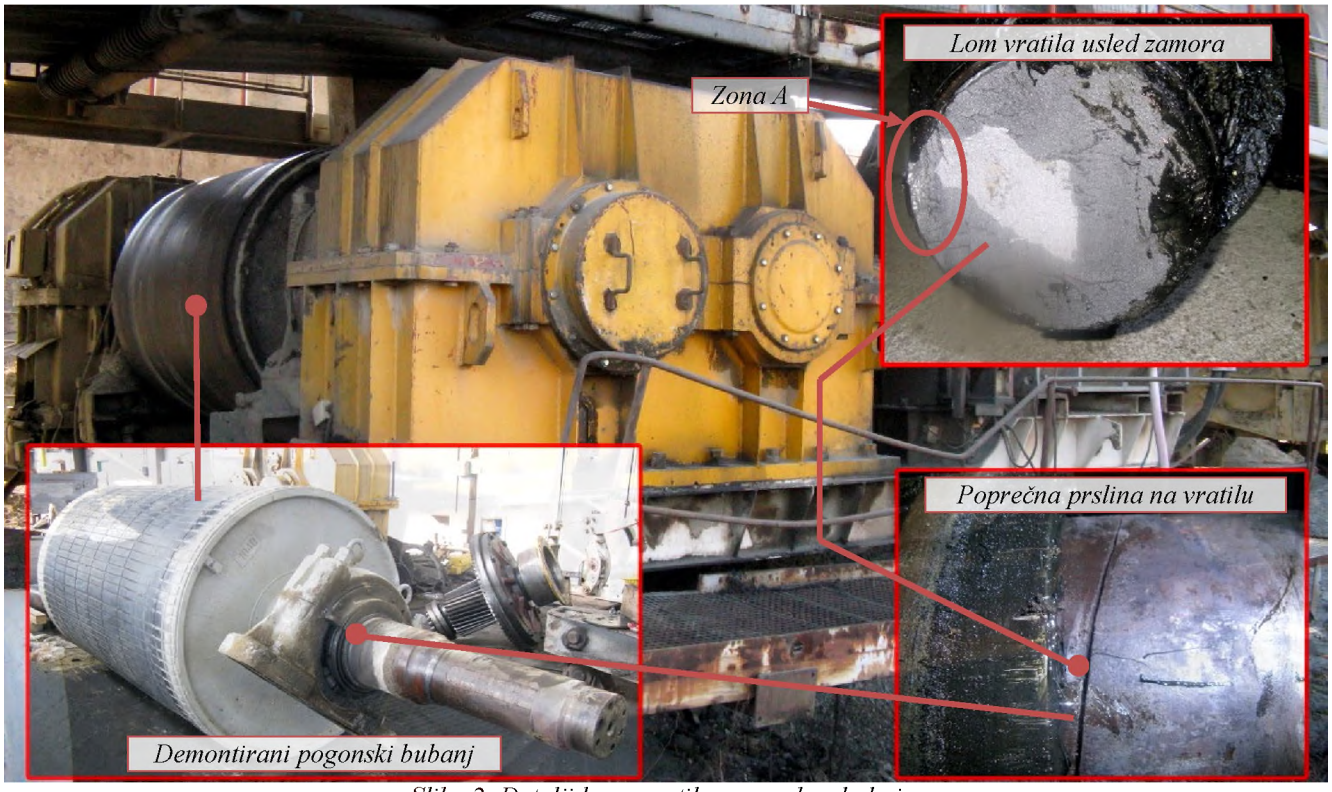

Slika 2: Detalji loma vratila pogonskog bubnja

2. ANALIZA NAPONA VRATILA

2.1. Opterećenje vratila pogonskog bubnja

Vratilo pogonskog bubnja, prikazano na Slici 3, opterećeno je redukovanim momentom savijanja uzrokovanim: sumom tereta na bubnju q_t, težinom samog bubnja q_b i zateznom silom od gumene trake F_r, na rastojanju l_g pa se njegova vrednost određuje na osnovu izraza:

$$M = \frac{(q_t + q_b + F_r)}{2} \cdot l_g, Nm \qquad (1)$$

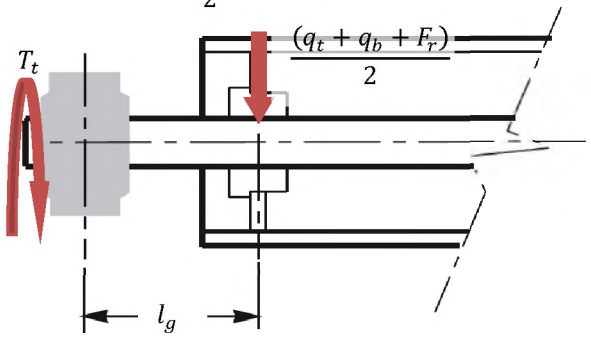

Slika 3: Redukovanje opterećenja pogonskog bubnja na vratilo

Težina tereta q_t je promenljiva veličina i zavisi od količine transportovanog materijala u trenutku vremena. U poređenju sa ostalim opterećenjima, ova veličina je beznačajno mala pa se može izuzeti.

Težina bubnja q_b isključivo zavisi od težine plašta bubnja, omotača, glavčine i ostalih delova bubnja. Usled velike sopstvene težine bubnja, ova veličina se mora uzeti u obzir.

Zatezna sila od gumene trake, kao najveća sila, se može podeliti na nailaznu F_1 i silaznuF_2 silu (Slika 4). Rezultanta ovih dveju sila F_r je najveća sila koja opterećuje vratilo na savijanje. Vrednost ove veličine je promenljiva u zavisnosti od datih uslova u eksploataciji. Npr. pri atmosferskim padavinama, usled vlažnosti između gumene trake i pogonskog bubnja, smanjuje se trenje, dolazi do proklizavanja pa se traka mora dodatno zategnuti. Zategnutost pri kojoj se može ostvariti kretanje trake je data Ojlerovom jednačinom, [8,9]:

$$\frac{F_1}{F_2} \leq e^{\mu\alpha} \qquad (2)$$

Iz jednačine (2) se zaključuje da zatezna sila eksponencijalno menja vrednost, pri čemu je μ koeficijent trenja između bubnja i trake koji zavisi od obvojnog ugla trake oko bubnja α.

Sa druge strane, da bi se pokrenula traka, ukupna vučna sila F_{b0} na obodu pogonskog bubnja mora biti jednaka razlici ovih dveju sila:

$$F_{b0} = F_1 - F_2 \quad (3)$$

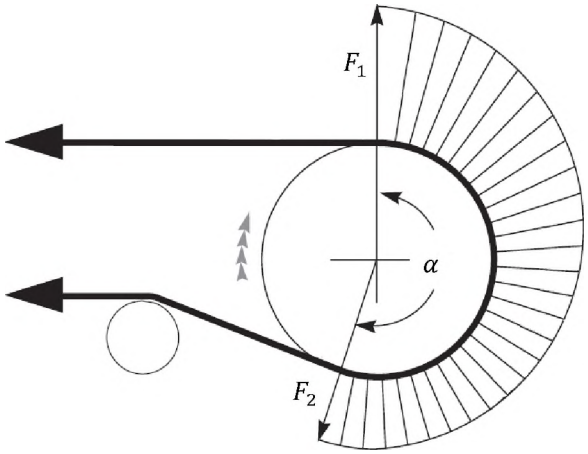

Slika 4: Nailzna i silazna zatezna sila od gumene trake

U zavisnosti od broja bubnjeva u pogonskoj jedinici, vrednosti zateznih sila se mogu odrediti na osnovu izvedenih izraza, [10]:

1. za jednobubanjske pogone:

$$F_1 = F_{b0} \cdot \left(1 + \frac{1}{e^{\mu\alpha} - 1}\right), N \quad (4)$$

$$F_r = \sqrt{F_1{}^2 + F_2{}^2 - 2 \cdot F_1 \cdot F_2 - cos\alpha}, N \quad (5)$$

2. za dvobubanjske pogone:

$$F_1 = F_{b0} \cdot \left(1 + \frac{1}{e^{(\mu_1\alpha_1 + \mu_2\alpha_2)} - 1}\right), N \quad (6)$$

$$F_r = F_1 \cdot \sqrt{1 + \frac{1}{e^{2\cdot\mu_1\alpha_1}} - 2\frac{cos\alpha_1}{e^{\mu_1\alpha_1}}}, N \quad (7)$$

Sve pomenute sile, koje nastaju na pogonskom bubnju, redukuju se na površinu povezivanja steznog prstena i vratila, što je prikazano Slikom 3. Zbog toga, obim savijanja zavisi od fleksibilnosti glavčine bubnja i veličine steznog prstena. Ako su stezni prsteni i glavčine prilično kruti, onda će dolaziti do savijanja vratila izvan bubnja.

Pored savijanja, vratilo pogonskog bubnja je opterećeno i momentom uvijanja od pogonske jedinice. Veličina torzionog momenta na rukavcu vratila, definiše se na osnovu efektivne snage motora P_{ef}:

$$T_t = \frac{P_{ef}}{\omega}, Nm \quad (8)$$

2.2. Analiza primenom metode konačnih elemenata

Modeli prikazani na Slici 5. predstavljaju dominantne pogonske bubnjeve na trakastim transporterima PK Drmno. Njih čine glavne komponente kao što su: vratila, plaštovi, glavčine, stezni prstenovi, kućišta ležaja i ležaji jer na krutost vratila utiču priključne komponente.

Veze između vratila i steznih prstenova, vratila i ležaja su modelirane kao vezni čvorovi, dok su ostale veze modelirane izjedna čime se sve ostale komponente bubnja objedinjuju.

Sa jedne strane vratila, uležištenja omogućavaju rotiranje i klizanje, dok sa suprotnih strana, uležištenja dozvoljavaju samo rotaciju.

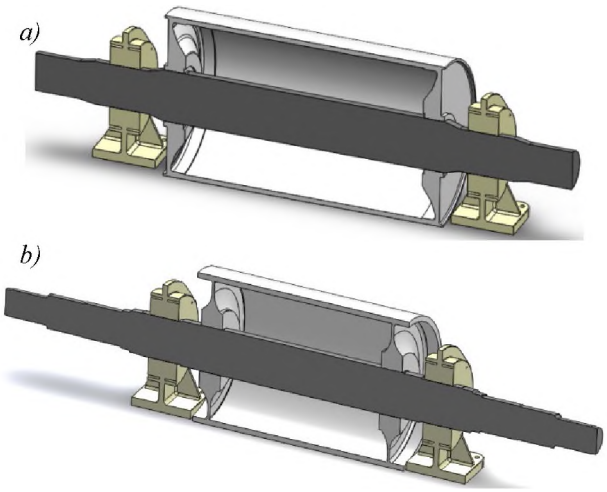

Slika 5: 3D modeli dominantnih bubnjeva

Nailazna zatezna sila od gumene trake, za normalne radne uslove, prema konstrukcionoj dokumentaciji, ima vrednost $F_1 = 1140\ kN$, dok vrednost silazne zatezne sile iznosi $F_1 = 640\ kN$. Obvojni ugao trake oko bubnja je 180 °, dok se bubanj okreća sa $59 min^{-1}$ pri instaliranoj snazi od 1000 kW [11].

Vratila su izrađena od niskolegiranog čelika 42CrMo4+QT visoke čvrstoće. Sama izrada se vrši kovanjem, a kasnije se podvrgavaju termičkoj obradi [11]. Pretpostavlja se da su materijali homogeni i izotropni, te da nema zaostalih naprezanja.

Trodimenzionalni modeli vratila diskretizovani su konačnim elementima tipa tetraedra posredstvom adaptivne metode koja pruža daleko tačnije rezultate u odnosu na korišćenje linearnih i paraboličkih konačnih elemenata. Parametri generisanih mreža dati su u Tabeli 1.

Tabela 1: Parametri generisanih mreža

Tip pogonskog bubnja	Broj čvorova	Broj konačnih elemenata
a)	187692	120912
б)	186367	119203

Detalj mreže, za pogonski bubanj *b)*, u zoni pojave prslina i pukotina prikazan je na Slici 6.

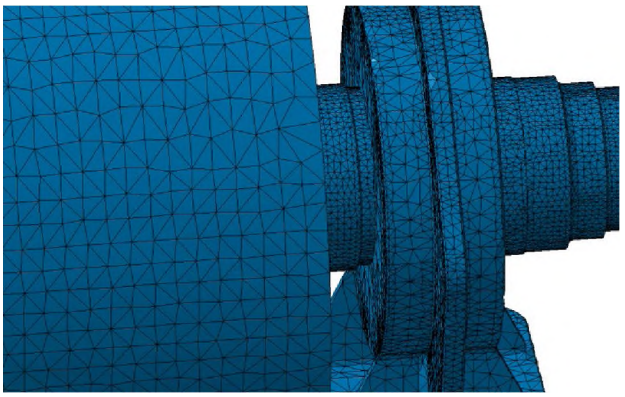

Slika 6: Mreža konačnih elemenatapogonskog bubnja u kritičnoj zoni

3.3 Analiza naponsko-deformacionog stanja

Deformacije vratila nastaju kao posledica redukovanja sila sa bubnja i usled momenta uvijanja od pogonske jedinice. Uvijanje ne izaziva velike deformacije, pa su shodno tome i posledice vrlo male. Daleko značajnije

posledice se ostvaruju pri savijanju. Ose vratila postaju prostorno krive linije pri kojima može doći do trajnih oštećenja vratila.

Na Slikama 7 i 8, gde su prikazani aksonometrijski izgledi deformisanih vratila (faktor uvećanja 100), može se primetiti da pod opterećenjem dolazi do deformisanja vratila i to na mestu između ležaja i bubnja. Ova pojava je uobičajena jer je direktna posledica promene prečnika vratila. Sva vratila sa izrazitim diskontinuitetima u veličinama poprečnog preseka, sa uzdužnim i poprečnim žlebovima, otvorima, čvrstim, neizvesnim i labavim naleganjima koja su potrebna za postavljanje i spajanje delova, sadrže izvore koncentracije napona već u neoštećenom stanju. Svako dodatno oštećenje kontaktne površine samo povećava vrednosti intenziteta ekvivalentnog napona.

Za tip pogonskog bubnja *a)*, gde je prelaz između prečnika vratila na mestu bubnja i rukavca za ležaj konusan (Slika 7), vrednost maksimalnog ekvivalentnog *von-Misses*-ov napona iznosi $\sigma_{vM,max} = 39{,}139\ MPa$.

Za tip pogonskog bubnja *b)*, gde je prelaz između prečnika vratila na mestu bubnja i rukavca za ležaj stepenast (Slika 8), vrednost maksimalnog ekvivalentnog *von-Misses*-ovog napona očekivano ima veću vrednost $\sigma_{vM,max} = 56{,}307\ MPa$.

Ukoliko bi se nastavilo sa povećanjem prelaza sa manjeg na veći prečnik, koncentracija napona bi se značajno smanjila. Ipak, mogućnost za to je ograničena jer preveliki prelazi odaljavaju bubanj od oslonaca.

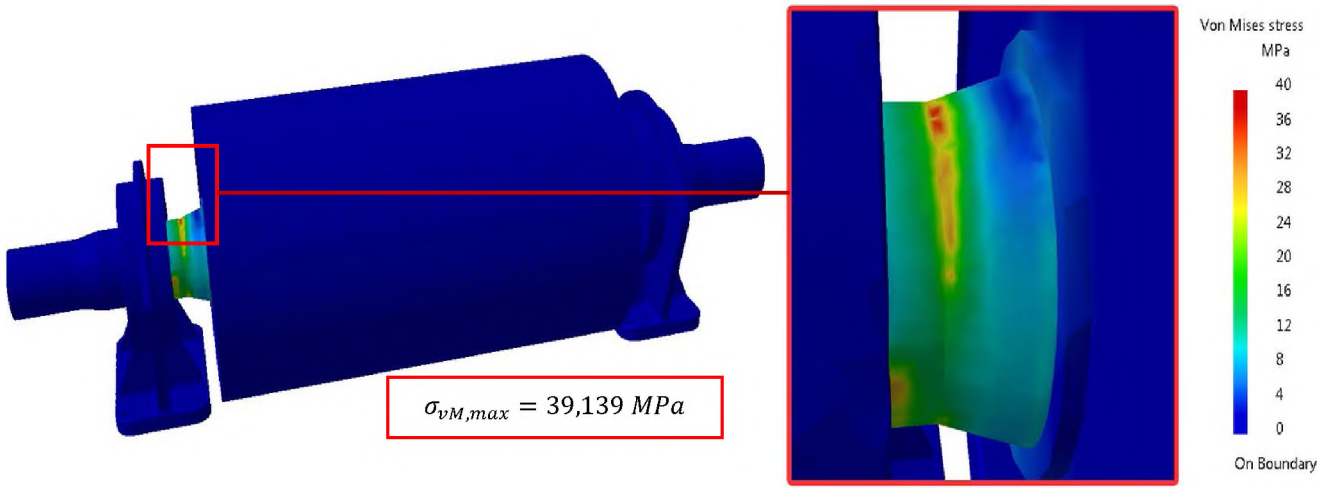

*Slika 7: Maksimalni ekvivalentni von-Misses-*ov *napon za tip pogonskog bubnja a)*

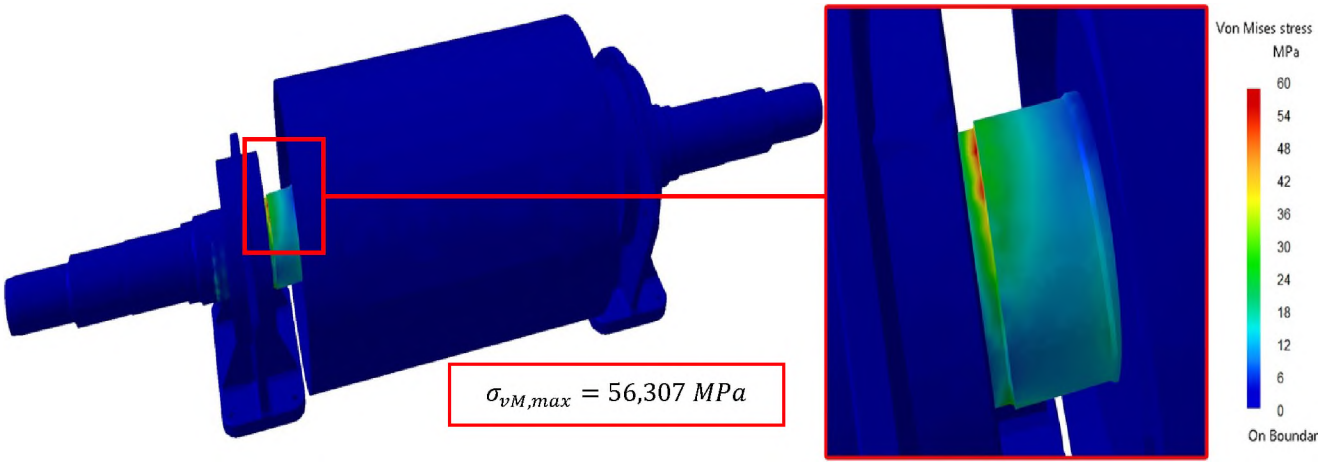

*Slika 8: Maksimalni ekvivalentni von-Misses-*ov *napon za tip pogonskog bubnja b)*

Na Slici 9 prikazani su rezultati maksimalnog ekvivalentnog *von-Misses*-ovog napona vratila u zavisnosti od povećanja veličine prelaznog radijusa r između manjeg prečnika konusa i rukavca za ležište (tip pogonskog bubnja *a*). Da bi se proverio uticaj promene veličine radijusa kod vratila izrazito velikih dimenzija, izvršene su dodatne simulacije vratila za više vrednosti radijusa, pored već proračunatog od 5 mm prema originalnoj tehničkoj dokumentaciji. Uočava se značajno smanjenje maksimalnog ekvivalentnog *von-Misses*-ovog napona sa povećanjem vrednosti radijusa r i zaključuje da svako zaobljenje smanjuje koncentraciju napona bez obzira na veličinu vratila.

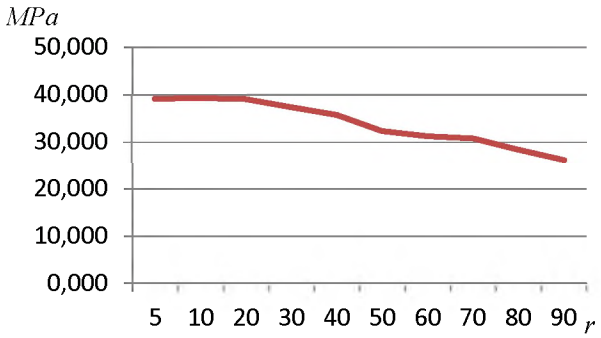

*Slika 9: Uticaj radijusa zaobljenja r na maksimalni ekvivalentni von-Misses-*ov *napon*

U cilju vizuelizacije polja pomeranja, koja su posledica opterećenja analiziranih vratila, na Slikama 10 i 11, prikazani su vektori translatornog pomeranja. Najveća pomeranja javljaju se shodno deformacijama, na mestima između ležišta i bubnja.

Analizirajući polja pomeranja na Slikama 10 i 11, očigledno je da se najveća pomeranja javljaju na jednom kraju vratila u gornjoj zoni, dok se na suprotnom kraju javljaju u donjoj zoni. To znači da jedna glavčina bubnja sa svojim unutrašnjim delom, na jednoj strani vrši pritisak na vratilo, dok suprotna strana ostaje manje opterećena.

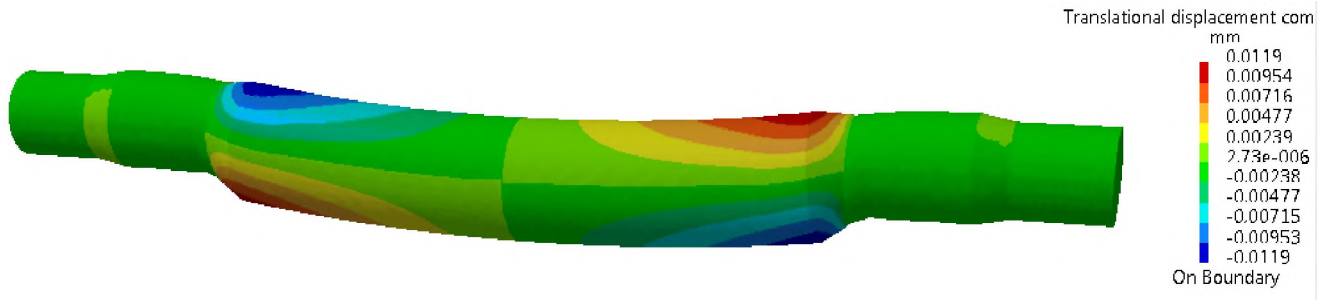

Slika 10: Polja pomeranja vratila pogonskog bubnja tipa a)

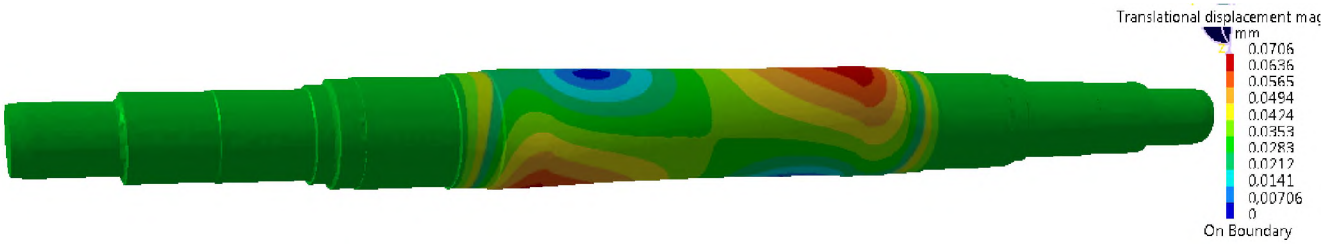

Slika 11: Polja pomeranja vratila pogonskog bubnja tipa b)

3.4 Diskusija rezultata

Analize napona primenom metode konačnih elemenata pokazuju da daleko bolju raspodelu napona imaju vratila sa konusima između steznih prstenova i ležaja u odnosu na vratila sa stepenastim prelazima. Izrada konusa u odnosu na stepenasti prelaz je daleko skuplja, ali zato omogućava prenošenje daleko većih radijalnih sila.

Pored konusa, glavčine na bubnju *a)* pružaju bolju krutost vratila i imaju bolju raspodelu napona u odnosu na glavčine na bubnju *b*), pa se ovaj pogonski bubanj može smatrati boljim konstrukcijskim rešenjem.

Dakle, pri rekonstrukciji postojećih i izgradnji novih sistema bolje je primenjivati bubnjeve sa T glavčinama, kao i vratila sa konusnim prelazima između steznog prstena i ležaja. Međutim, analize napona takođe pokazuju da su vrednosti napona dobijene u vratilima na mestu otkaza preniske da bi dovele do oštećenja vratila lomom usled preopterećenja. Maksimalna vrednost napona, dobijena analizom, je mnogo manja od dozvoljenih vrednosti za dati materijal.

4. DODATNI FAKTORI KOJI UTIČU NA KONCENTRACIJU NAPONA

Dalja istraživanja navode na zaključak da do otkaza vratila može doći usled zamora jer se ovakvi lomovi javljaju pri znatno manjim naponima od dozvoljenih.

Pošto su elementi pogonskog bubnja postavljeni na vratilo na kontaktnim površinama, u toku teške eksploatacije može doći do pomeranja površinskih slojeva materijala, a kao posledica stalnog pomeranja dolazi do zamora materijala.

Ako vrednosti naprezanja prelaze granicu tečenja materijala, razvoj oštećenja i konačan lom nastupaju već nakon relativno niskog broja ciklusa opterećenja. U tom slučaju reč je o tzv. niskocikličnom zamoru materijala. Međutim, zamor materijala i njime uzrokovan konačni lom mogu biti izazvani i cikličnim opterećenjima koja u materijalu uzrokuju nazivna naprezanja čije su vrednosti niže od granice tečenja materijala. Takav se oblik zamora naziva visokocikličnim zamorom materijala, [5].

Na lom vratila može uticati i povećanje ugiba do koga dolazi pri velikom zatezanju trake. U takvim slučajevima potrebno je proveriti ispravnost uređaja za merenje zatezanja trake-tonometra.

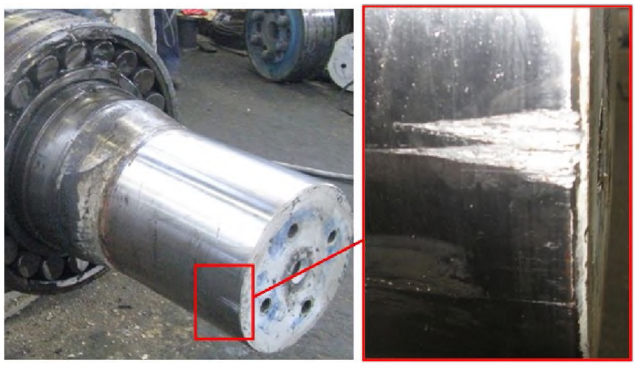

Slika 12: Oštećenje vratila pogonskog bubnja usled zamene krute spojnice

Takođe, sva oštećenja vratila u vidu zareza, riseva i brazda (Slika 12) nastala na mestima ugrađenih delova, kao što su, ležaji, stezni prstenovi i spojnice, regenerišu se zavarivanjem, a zatim se ponovo mašinski obrađuju. Sam proces zavarivanja dovodi do zaostalih napona koji se moraju eliminisati otpuštanjem.

Ne treba zanemariti i neuravnoteženost mase bubnja, koja može dovesti do neravnomernog opterećenja. Neuravnoteženost se eliminiše pravilnim balansiranjem i postavljanjem tegova na glavčini bubnja kao što je prikazano Slikom 13.

Slika 13: Dodavanje tegova na glavčini bubnja kako bi se eliminisala neuravnoteženost mase

Nakon svakog postupka montaže, neophodno je kontrolisati da li dolazi do poremećaja centričnosti spojnice ili ležaja.

Pored svega ovog, u materijalu vratila koje se izrađuje kovanjem mogu nastati greške. Česte greške prilikom kovanja su preklapanje materijala i stvaranje dvoslojnosti, što zapravo znači pojavu skrivene pukotine na mestu preklopa. Temperature kovanja nisu dovoljno visoke da bi na mestima preklopa, pod delovanjem udarca, dovele do zavarivanja preklopnih spojeva, [12].

Svi nabrojani potencijalni poremećaji mogu biti uzroci povećanja maksimalnog ekvivalentnog *von-Misses*-ovog napona i konačnog loma, koji dovode do otkaza čitavog pogonskog bubnja.

5. ZAKLjUČAK

Rezultati dobijeni analizom naponsko-deformacionog stanja vratila pogonskog bubnja u softverskom paketu *Catia* pokazuju da su vrednosti maksimalnih ekvivalentnih *von-Misses*-ovih napona neoštećenih homogenih vratila izuzetno male ($39{,}139\ MPa$ i $56{,}307\ MPa$) da bi dovele do oštećenja vratila lomom usled preopterećenja.

Takođe, analize pokazuju da daleko bolju raspodelu opterećenja imaju vratila sa konusom između steznog prstena i ležaja ($39{,}139\ MPa$) u odnosu na vratila sa stepenastim prelazima ($56{,}307\ MPa$) i da pri rekonstrukciji postojećih i izgradnji novih sistema bolje je primenjivati bubnjeve sa T glavčinama, kao i vratila sa konusnim prelazom.

Dalja istraživanja navode na zaključak da uzroke povećanja koncentracije napona i otkaza vratila treba tražiti u zamoru, zatim u plastičnim deformacijama koje se mogu uzrokovati velikim zatezanjem, zaostalim naponima posle reparacije vratila, neuravnoteženosti mase bubnja, greškama u materijalu vratila koje se izrađuje kovanjem, poremećajima centričnosti spojnice i ležaja prilikom postupka montaže i drugim relevantim faktorima.

LITERATURA

[1] T. J. King, "The Function and Mechanism of Conveyor Pulley Drums", Beltcon 4th conference, Johannesburg, (1985)

[2] C. P. Prasad, S. M. Jadhav, "Redesigning & Optimization of Conveyor Pulley", Ijltemas, Volume 4, pp. 28-33, (2015)

[3] X. Oscar fenn Daniel, A. Hussain lal, "Stress Analysis in Pulley of Stacker-Reclaimer by Using Fem Vs Analytical", Journal of Mechanical and Civil Engineering (IOSR-JMCE), Volume 12, pp. 52-59, (2015)

[4] C. Affolter, G. Piskoty, R. Koller, M. Zgraggen, T. F. Rütti, "Fatigue in the shell of a conveyor drum", Engineering Failure Analysis, Volume 14, pp.1038-1052, (2007)

[5] D. Momčilović, R. Mitrović, I. Atanasovska, "Koncentracija napona i zamor materijala - savremeni pristup proračunu mašinskih elemenata i konstrukcija", Univerzitet u Beogradu - Mašinski fakultet, Beograd, (Srbija), (2016)

[6] D. Momčilović, "Razvoj metoda za povećanje radnog veka i pouzdanosti mašinskih sistema u uslovima zamora", Doktorska disertacija, Mašinski fakultet Univerziteta u Beogradu (Srbija), (2014)

[7] J. Schijve, "Fatigue of Structures and Materials", Springer Netherlands, New Delhi (India), (2009)

[8] https://www.rulmecacorp.com/Conveyor_Idler_Roller_catalog/Complete_Idler_Roller_Catalog.pdf

[9] http://www.roxon.sandvik.com/sandvik/1182/Internet/SandvikMsHandling/Roxon/FI05019.nsf/LookPortal/Portal62E328175D0E9113C22570C50037741E/$file/4-eng.pdf

[10] I. Trešćec, "Teorija, proračun i primena transportera s gumenom trakom", Zavod za produktivnost, Zagreb, (Hrvatska), (1983)

[11] Available documentation on belt conveyors at the open pit surface mine "Drmno"

[12] K. Lange (Ed.), "Handbook of Metal Forming", McGraw-Hill, New York, (USA), (1985)

IMK-14 – Research & Development in Heavy Machinery 25(2019)3, EN 69-74
UDC 621 ISSN 0354-6829

Stress–Strain Analysis of Conveyor Drive Pulley Shaft

Milan P. Vasić[1], Zorica D. Đorđević[1], Mirko Ž. Blagojević[1]*
[1] University of Kragujevac, Faculty of Engineering, Kragujevac (Serbia)

The paper presents an analysis of the stress deformation state of shafts of characteristic drive pulleys on belt conveyors in Drmno open pit mine. The shape and dimensions of the shafts were defined based on the original technical documentation, and the stress state was verified by applying the finite difference method in the Catia software package. Loads were simulated for real working conditions in exploitation. The analysis results showed that shafts with cone between locking device and bearing have the best load distribution and that T-shaped end disks most favourably transfer loads to the shaft. The analyses also showed that the values of stresses formed in shafts at the failure site are not high enough to lead to shaft failure due to overload and that failure cause should be sought in fatigue, then in plastic deformation, residual stresses after shaft repair and pulley weight unbalance.

Keywords: Drive pulleys, Shafts, Stress–strain analysis

1. INTRODUCTION

Belt movement on belt conveyors is accomplished by one or more drive pulleys, with shafts, among other things, playing a special role and being of particular importance. They receive the entire load from belt conveyors and drive units, and rest upon only two axial-radial bearings.

Normally, a drive pulley, as a complex technical system (Figure 1), consists of: end disk (1), shell (2), lagging (3), shaft (4), locking device (5), bearing housing (6), bearing (7), rigid flange coupling (8) or another bond with gearbox.

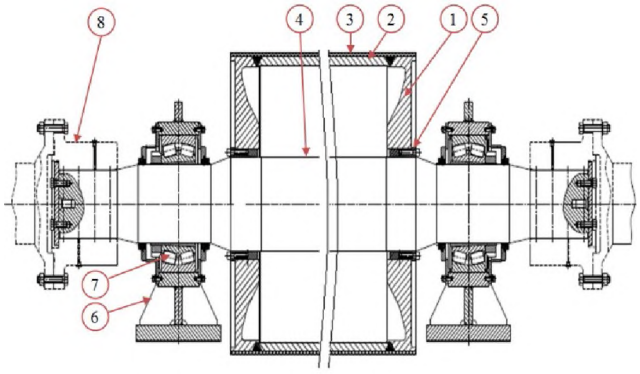

Figure 1: Basic components of a drive pulley

Over many years of exploitation, Drmno open-pit mine has been facing cracks and fissures in the structure of the drive unit shafts, resulting in system slowdown. The failures are most often located in the area between the locking device and bearing.

Each delay of this system brings high financial losses, and especially coal systems negatively affect the operation of thermal power plants, creating problems in the delivery of fuels to power plants. If the thermal power plant and the mine do not have a spare way of delivering coal in a certain quantity and at a certain pace, successive system delays may cause the entire power plant falling out of the power grid.

Literature research has shown that in addition to marked discontinuities in cross-section sizes, the end disk design also affects the service life of a shaft.

On the basis of a large number of analyses, King suggested the use of T-shaped end disks instead of those L-shaped, as they minimize the cost of machining while reducing the stress of welds [1].

Pol and Jadhav optimized the radius values of shaft rounding at the point of transition from the diameter upon which the locking device rests to the diameter of bearing resting spot, as well as the values of shell wall thickness. Thus, for the ⌀ 100 *mm* shaft, they reduced the stress value by 9% [2].

Oscar and Hussain analysed the stress of a pulley on a bucket-wheel excavator [3]. They managed to reduce the stress value of the shaft by a more even distribution of load, which was achieved by inserting more middle disks (supports) inside the pulley.

A group of authors studied the failure of pulley welds and the application of necessary reinforcements between the end disk and the shell [4]. They concluded that initial loading can be crucial to the pulley service life.

Based on the literature review, it can be concluded that there is interdependence between the pulley components since all loads are reduced to the shaft.

It should also be borne in mind that shaft service life is affected by improper mounting. Any disturbance of centricity, even a very small one, leads to cyclic stress, i.e. premature fatigue. In addition, one should not overlook the great tension that occurs when the belt slips around the drive pulley.

Therefore, the paper aims to analyse the individual shaft stress and deformation states for the types of drive pulleys that are most often applied in Drmno open-pit mine and to point to potential shortcomings as well as good solutions to be applied in the construction of new systems.

Comparative modal analysis of the shaft was performed for two dominant types of drive pulleys the components of which were modelled based on the original technical documentation in Catia software.

*Corresponding author: Faculty of Engineering, Kragujevac, Sestre Janjic 6, Serbia, mirkob@kg.ac.rs

2. DESCRIPTION OF FAILURES

Shaft fracture may result from overload, plastic deformations, or fatigue, and each type of fracture is determined by the fracture surface appearance [5].

In case of overload, the crack develops constantly, and the fracture surface is relatively coarse.

In the case of fatigue-induced shaft fracture, the crack growth rate is not constant, so the fracture surface is relatively smooth – matte, and the final fracture is relatively coarse, coarse-grained and rough [6,7].

An example of such a fracture is shown in Figure 2. Visual inspection reveals a characteristic part of the fracture surface, called zone A, which is rough and is the final fracture that occurred when the cross-section surface was reduced so much that it could no longer withstand the rated load. The rest of the fracture surface is smooth.

Generally, fractures due to flexural stress are perpendicular to the shaft axis of the, just as in Figure 2, while fractures resulting from torsion stress are often set at an angle of 45 ° to the shaft axis

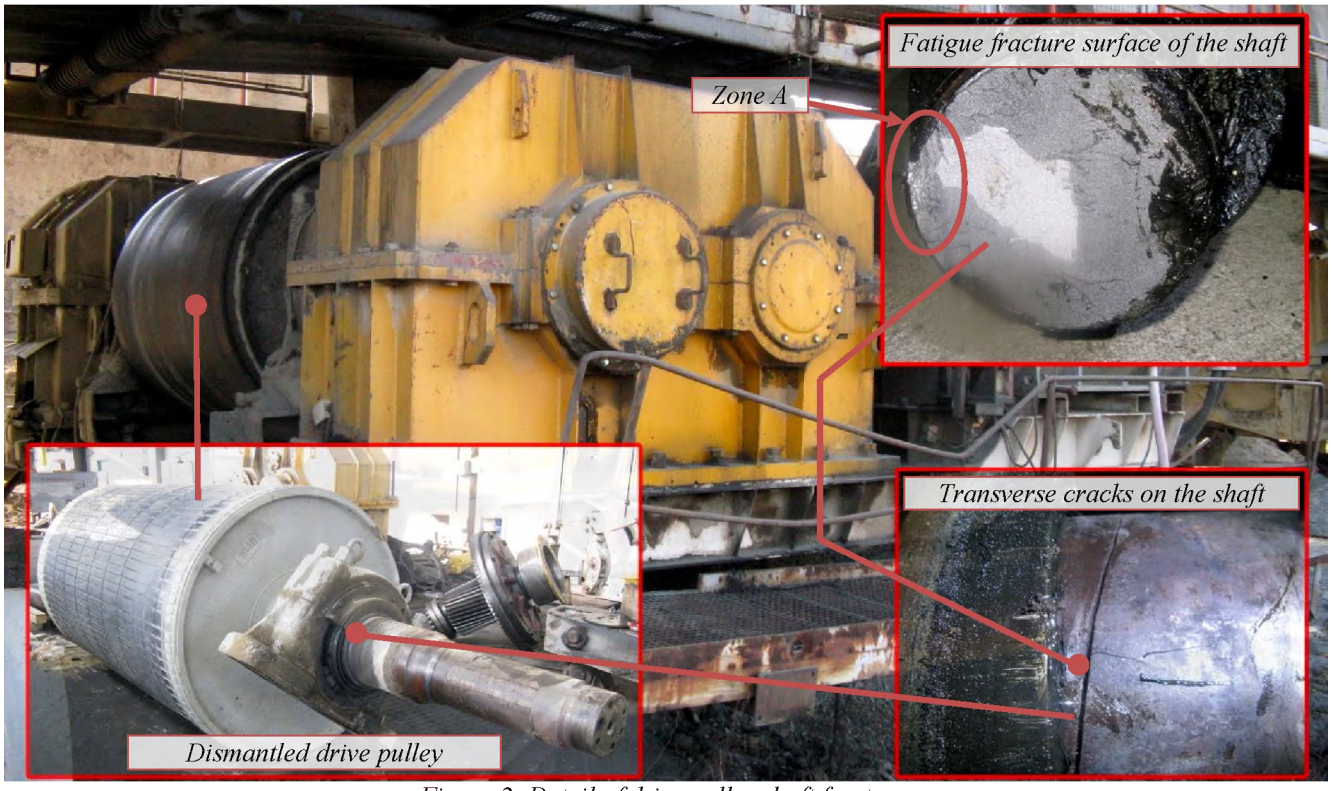

Figure 2: Detail of drive pulley shaft fracture

3.SHAFT STRESS ANALYSIS

3.1. Drive pulley shaft load

The drive pulley shaft, shown in Figure 3, is loaded by the reduced bending moment caused by the sum of loads on the pulley q_t, the weight of the pulley itself q_b and total belt tension F_r , at a distance l_g so its value is determined as follows:

$$\mathrm{M} = \frac{(q_t + q_b + F_r)}{2} \cdot l_g, Nm \qquad (1)$$

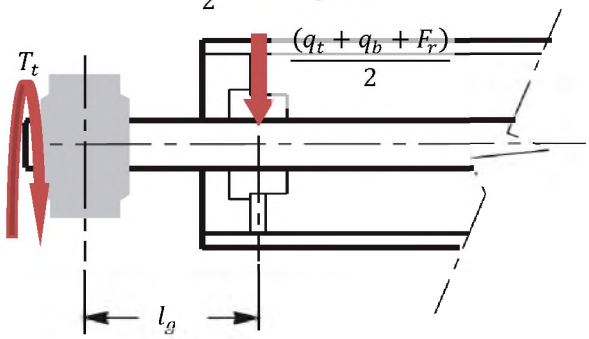

Figure 3: Reducing drive pulley load to the shaft

The weight of load q_t is a variable size and depends on the amount of material transported at a given time. Compared to other loads, this size is insignificantly small, so it can be excluded.

The weight of the pulley, q_b depends solely on the weight of the pulley shell, lagging, end disk and other parts of the pulley. Due to the great weight of the pulley, this size must be allowed for.

Total belt tension, as the greatest force, can be divided into tight side F_1 and output side F_2 force (Figure 4). The resultant of these two forces, F_r is the greatest force that loads the shaft to bending. The value of this size is variable depending on the given conditions in exploitation. For example, at atmospheric precipitation, due to humidity between the belt and the drive pulley, friction is reduced, leading to slippage, so the belt must be further tightened. Tension at which belt movement can be achieved is given by the Euler equation [8, 9]:

$$\frac{F_1}{F_2} \leq e^{\mu\alpha} \qquad (2)$$

From equation (2), it is concluded that the tensile force exponentially changes the value, with μ being the coefficient of friction between the pulley and the belt, which depends on the pulley wrap angle α.

On the other hand, in order to move the belt, required periphery tractive force F_{b0} on the drive pulley must be equal to the difference between these two forces:

$$F_{b0} = F_1 - F_2 \quad (3)$$

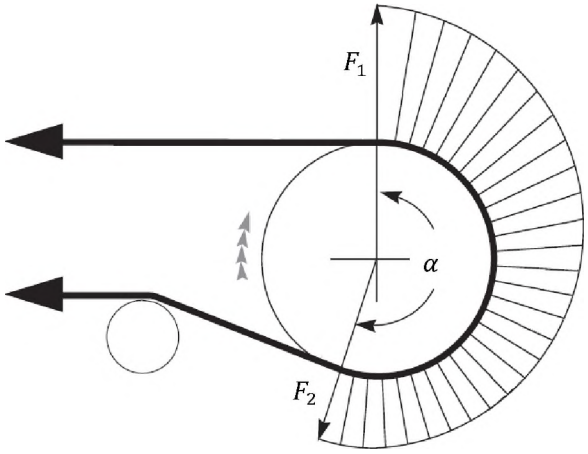

Figure 4: Belt tight side and output side forces

Depending on the number of pulleys in the drive unit, the values of the tensile forces may be determined from the derived expressions [10]:

1. for one pulley drives:

$$F_1 = F_{b0} \cdot \left(1 + \frac{1}{e^{\mu\alpha} - 1}\right), N \quad (4)$$

$$F_r = \sqrt{F_1{}^2 + F_2{}^2 - 2 \cdot F_1 \cdot F_2 - cos\alpha}, N \quad (5)$$

2. for dual pulley drives:

$$F_1 = F_{b0} \cdot \left(1 + \frac{1}{e^{(\mu_1\alpha_1 + \mu_2\alpha_2)} - 1}\right), N \quad (6)$$

$$F_r = F_1 \cdot \sqrt{1 + \frac{1}{e^{2\cdot\mu_1\alpha_1}} - 2\frac{cos\alpha_1}{e^{\mu_1\alpha_1}}}, N \quad (7)$$

All of the forces mentioned, formed on the drive pulley, are reduced to the connection surface of the locking device and the shaft, as shown in Figure 3. Therefore, the extent of bending depends on the flexibility of the pulley end disk and the size of the locking device. If the locking devices and end disks are quite rigid, then the shafts will bend outside the pulley.

Apart from being loaded by bending, the drive pulley shaft is loaded with the twisting moment from the drive unit. The size of the moment of torsion on the shaft sleeve is defined based on the effective power of the engine P_{ef}:

$$T_t = \frac{P_{ef}}{\omega}, Nm \quad (8)$$

3.2. Analysis using the finite element method

The models shown in Figure 5 represent the dominant drive pulleys on the Drmno open pit mine belt conveyors. They consist of the major components such as shafts, shells, end disks, locking devices, bearing housings and bearings as the shaft rigidity is influenced by the connecting components.

The connections between shafts and locking devices, and shafts and bearings, are modelled as tie knots, while the other connections are modelled integrally, bringing all other pulley components together.

On one side of the shaft, the bearings allow rotation and sliding, while on the opposite sides, the bearings allow only rotation.

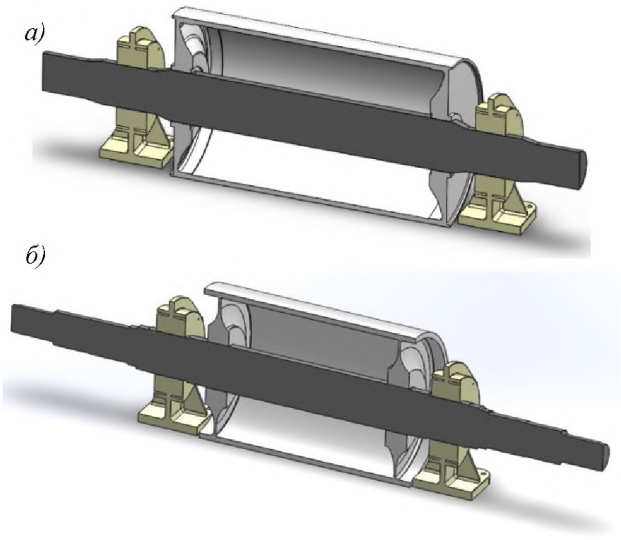

Figure 5: 3D models of dominant pulleys

The tight side force of the belt, for standard operating conditions, according to the design documentation, has a value of $F_1 = 1140\ kN$, while the output side force is $F_1 = 640\ kN$. The pulley wrap angle is 180°, while the pulley rotates at 59 min^{-1} at 1000 kW of installed power [11].

The shafts are made of low alloy 42CrMo4 + QT steel of high strength. They are made by forging and later subjected to heat treatment [11]. It is assumed that the materials are homogeneous and isotropic and that there are no residual stresses.

Three-dimensional shaft models are discretized with tetrahedral finite elements by means of the adaptive method that provides far more accurate results compared to linear and parabolic finite elements. The parameters of the generated meshes are given in Table 1.

Table 1: Parameters of generated meshes

Drive pulley type	Number of nodes	Number of finite elements
a)	187692	120912
б)	186367	119203

Detail of the mesh, for the drive pulley b), in the zone of cracking and fissuring, is shown in Figure 6.

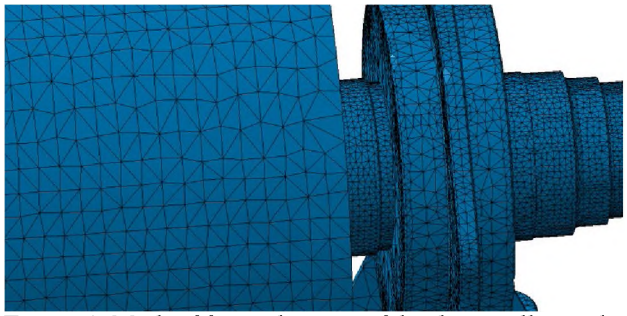

Figure 6: Mesh of finite elements of the drive pulley in the critical zone

3.3 Analysis of stress deformation state

Shaft deformations are caused by the reduction of forces from the pulley and by the twisting moment of the drive unit. Twisting does not cause large deformations, and consequently, the effects are very small.

Far more significant effects are achieved at bending. Shaft axes become spatially curved lines which can lead to permanent damage to the shaft.

In Figures 7 and 8, showing axonometric views of deformed shafts (magnification factor 100), it can be observed that, under load, a shaft gets deformed at a position between the bearing and the pulley. This phenomenon is common as it directly results from changing the shaft diameter. All shafts with pronounced discontinuities in cross-sectional sizes, with longitudinal and transverse grooves, openings, interference, clearance and slip fits required for mounting and joining parts, contain sources of stress concentrations already in the intact state. Any additional damage to the contact surface only increases the intensity values of the equivalent stress.

For a) type drive pulley, where the transition between the shaft diameter at the pulley site and the bearing sleeve is conical (Figure 7), the value of the maximum equivalent von Mises stress is $\sigma_{vM,max} = 39{,}139\ MPa$.

For b) type drive pulley, where the transition between the shaft diameter at the pulley site and the bearing sleeve is stepped (Figure 8), the value of the maximum equivalent von Mises stress expectedly has a higher value $\sigma_{vM,max} = 56{,}307\ MPa$.

If the transition from the smaller to the larger diameter continued to increase, the stress concentration would decrease significantly. However, the possibility of this is limited as too large transitions distance the pulley from the supports.

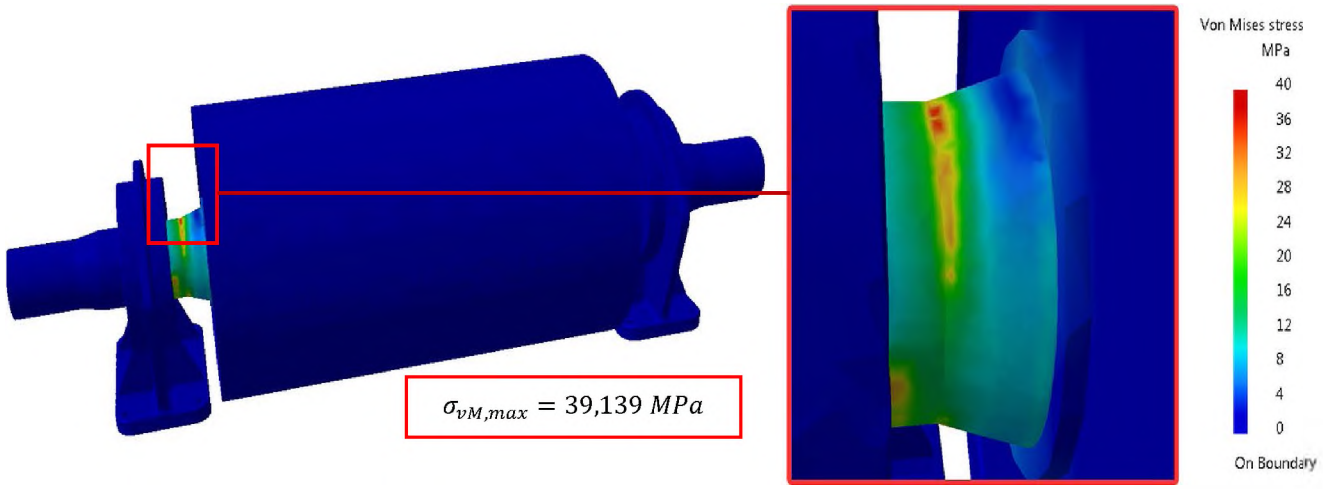

Figure 7: Maximum equivalent von Mises stress for a) type drive pulley

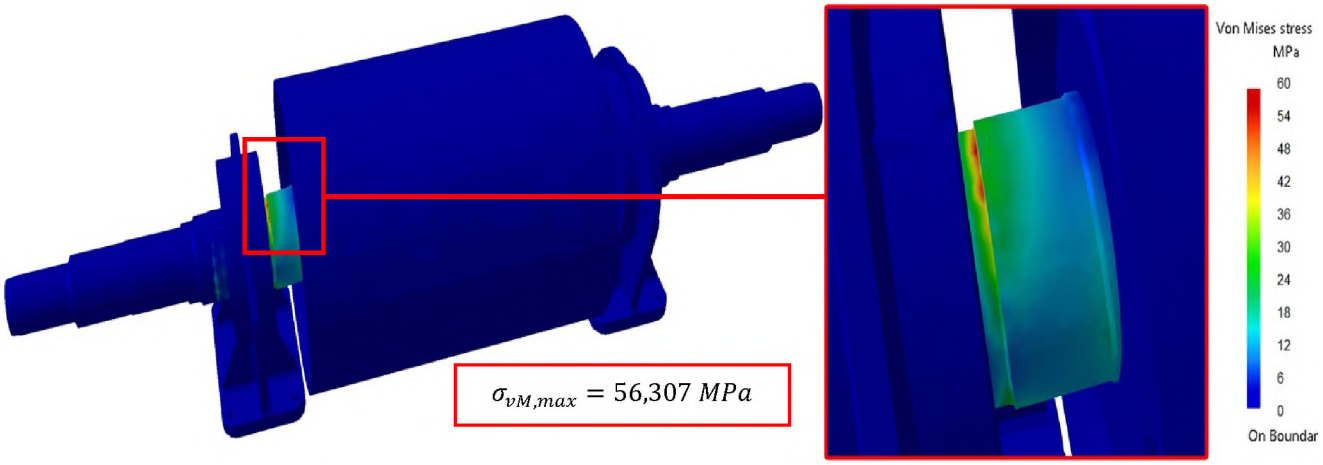

Figure 8: Maximum equivalent von Mises stress for b) type drive pulley

Figure 9 shows the results of the maximum equivalent von Mises stress of shaft depending on the increase in the size of the transition radius r between the smaller diameter of the cone and the bearing sleeve (type a drive pulley). In order to check the effect of changing the size of the radius on shafts of extremely large dimensions, additional shaft simulations were performed for several radius values, in addition to the already calculated 5 *mm* according to the original technical documentation. A significant decrease in the maximum equivalent von Mises stress with increasing radius r value is observed, so it is concluded that each rounding decreases the stress concentration regardless of the shaft size.

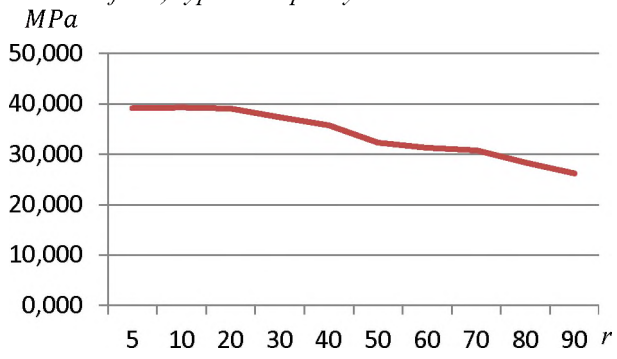

Figure 9: Effect of the rounding radius r on the maximum equivalent von Mises stress

In order to visualize the displacement fields resulting from the load of the analyzed shafts, translational displacement vectors are shown in Figures 10 and 11. Greatest displacements occur in line with deformations, in the places between the bearing and the pulley.

By analyzing the displacement fields in Figures 10 and 11, it becomes evident that the greatest displacements occur at one end of the shaft in the upper zone, while at the opposite end they occur in the lower zone. This means that one end disk of the pulley, with its inner part, exerts pressure on the shaft on one side, while the opposite side remains less loaded.

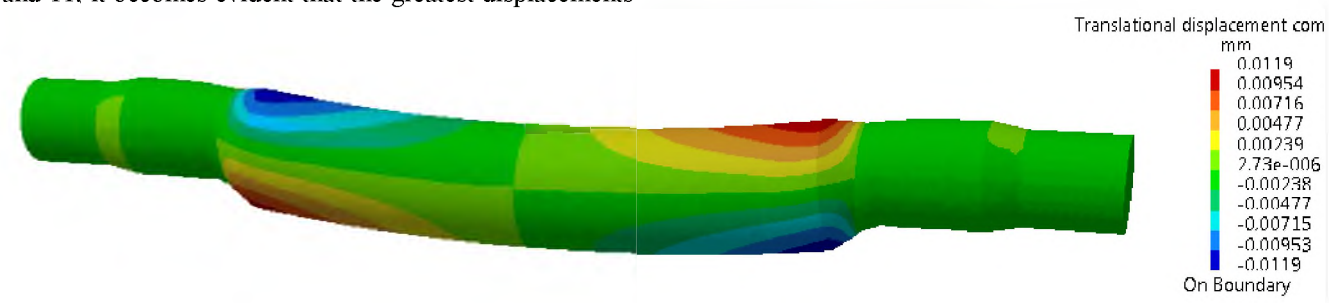

Figure 10: Displacement fields of type a) drive pulley shaft

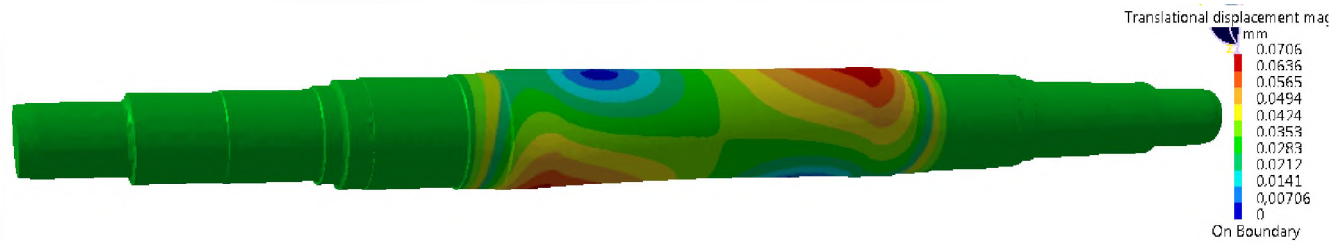

Figure 11: Displacement fields of type b) drive pulley shaft

3.4 Discussion

The stress analyses using the finite element method show that the shafts with cones between the locking devices and the bearing have a much better stress distribution than the shafts with stepped transitions. Constructing a conical is far more expensive compared to a stepped transition, but allows the transmission of far greater radial forces.

In addition to the cone, the end disks on the pulley a) provide better shaft rigidity and have a better stress distribution than the end disks on the pulley b), so this drive pulley can be considered a better structural solution.

Therefore, it is better to use T-shaped end disk pulleys, as well as shafts with conical transitions between the locking device and the bearing, when reconstructing existing and building new systems. However, stress analyses also show that the stress values obtained in the shaft at the failure site are too low to cause damage to the shaft by fracture due to overload. The maximum stress value obtained by the analysis is much lower than the permitted values for the given material.

4. ADDITIONAL FACTORS AFFECTING STRESS CONCENTRATION

Further research suggests that shaft failure can result from fatigue as such fractures occur at much lower stresses than permitted.

As the drive pulley elements are mounted on the shaft on the contact surfaces, the superficial layers of the material may be displaced during heavy exploitation, and material fatigue may occur as a result of constant displacement.

If the stress values exceed the material flow limit, the damage and eventual fracture develop after a relatively low number of load cycles. In this case, it is the so-called low-cycle fatigue of material. However, material fatigue and the resulting eventual fracture can also be caused by cyclic loads that cause in the material nominal stresses the values of which are lower than the material flow limit. This form of fatigue is called high-cycle fatigue of material [5].

Shaft fracture can also be affected by the increase in bending caused by high belt tension. In such cases, it is necessary to check the functionality of the device for measuring belt tension - trummeter.

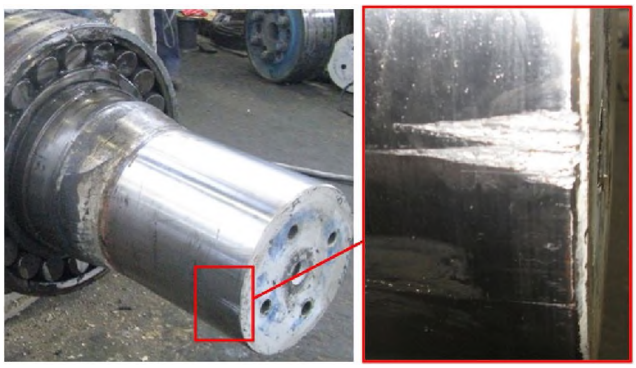

Figure 12: Damage to the drive pulley shaft due to replacement of rigid flange coupling

Also, all damages to the shaft in the form of notches, fissures, and grooves (Figure 12) occurring at the places of mounted parts, such as bearings, locking devices and couplings, are regenerated by welding and then re-machined. The welding process itself causes residual stresses that must be eliminated by relief.

One should also not neglect the unbalance of the pulley weight, which may lead to uneven load. Unbalance is eliminated by proper balancing and placing weights on the pulley end disk, as shown in Figure 13.

Figure 13: Adding weights on pulley end disk to eliminate weight unbalance

After each mounting procedure, it is necessary to control whether there is disturbance to the centricity of the coupling or bearing.

In addition, forged shaft material may also develop defects. Common defects resulting from forging are material overlapping and creation of double layer endless, which actually means appearance of a hidden crack at the overlapping site. Forging temperatures are not high enough to bring about welding of overlapping joints under the effect of an impact [12].

All of the listed possible disturbances may be the causes of the increase in the maximum equivalent von Mises stress and eventual fracture, leading to the failure of the entire drive pulley.

5. CONCLUSION

The results obtained by the analyses of the stress deformation state of the drive pulley shaft in the Catia software package show that the values of the maximum equivalent von Mises stresses of non-damaged homogeneous shafts are extremely low (39,139 MPa and 56,307 MPa) to result in fracture damage to the shaft due to overload.

Also, the analyses shows that the shaft with a cone between the locking device and the bearing (39,139 MPa) has a much better distribution of load than stepped transition shafts (56,307 MPa) and that it is better to apply T-shaped end disk pulleys as well as conical transition shafts when reconstructing the existing and building new systems.

Further research suggests that the causes of the increase in the stress concentration and shaft failure should be sought in fatigue, then in plastic deformations that can be caused by heavy tension, residual stresses after shaft repair, shaft weight unbalance, and defects in the material of the shaft made by forging, disturbances to the centricity of the coupling and bearing resulting from mounting procedure and other relevant factors.

REFERENCES

[1] T. J. King, "The Function and Mechanism of Conveyor Pulley Drums", Beltcon 4th conference, Johannesburg, (1985)

[2] C. P. Prasad, S. M. Jadhav, "Redesigning & Optimization of Conveyor Pulley", Ijltemas, Volume 4, pp. 28-33, (2015)

[3] X. Oscar fenn Daniel, A. Hussain lal, "Stress Analysis in Pulley of Stacker-Reclaimer by Using Fem Vs Analytical", Journal of Mechanical and Civil Engineering (IOSR-JMCE), Volume 12, pp. 52-59, (2015)

[4] C. Affolter, G. Piskoty, R. Koller, M. Zgraggen, T. F. Rütti, "Fatigue in the shell of a conveyor drum", Engineering Failure Analysis, Volume 14, pp.1038-1052, (2007)

[5] D. Momčilović, R. Mitrović, I. Atanasovska, "Koncentracija napona i zamor materijala - savremeni pristup proračunu mašinskih elemenata i konstrukcija", Univerzitet u Beogradu - Mašinski fakultet, Beograd, (Srbija), (2016)

[6] D. Momčilović, "Razvoj metoda za povećanje radnog veka i pouzdanosti mašinskih sistema u uslovima zamora", Doktorska disertacija, Mašinski fakultet Univerziteta u Beogradu (Srbija), (2014)

[7] J. Schijve, "Fatigue of Structures and Materials", Springer Netherlands, New Delhi (India), (2009)

[8] https://www.rulmecacorp.com/Conveyor_Idler_Roller_catalog/Complete_Idler_Roller_Catalog.pdf

[9] http://www.roxon.sandvik.com/sandvik/1182/Internet/SandvikMsHandling/Roxon/FI05019.nsf/LookPortal/Portal62E328175D0E9113C22570C50037741E/$file/4-eng.pdf

[10] I. Trešćec, "Teorija, proračun i primena transportera s gumenom trakom", Zavod za produktivnost, Zagreb, (Hrvatska), (1983)

[11] Available documentation on belt conveyors at the open pit surface mine "Drmno"

[12] K. Lange (Ed.), "Handbook of Metal Forming", McGraw-Hill, New York, (USA), (1985)